Expanding the spectrum of *PEX16* mutations and novel insights into disease mechanisms

Kishore R. Kumar[a,b,*,1], Gautam Wali[b,1], Ryan L. Davis[b], Amali C. Mallawaarachchi[c], Elizabeth E. Palmer[c,d,e,f], Velimir Gayevskiy[a], Andre E. Minoche[a], David Veivers[g], Marcel E. Dinger[a,h], Alan Mackay-Sim[i], Mark J. Cowley[a,h], Carolyn M. Sue[b]

[a] Kinghorn Centre for Clinical Genomics, Garvan Institute of Medical Research, Sydney, NSW, Australia
[b] Department of Neurogenetics, Kolling Institute, Royal North Shore Hospital, St. Leonards, NSW, Australia
[c] Garvan Institute of Medical Research, Sydney, NSW, Australia
[d] Sydney Children's Hospital, Randwick, NSW, Australia
[e] School of Women's and Children's Health, UNSW Medicine, The University of New South Wales, Sydney, NSW, Australia
[f] Genetics of Learning Disability Service, Waratah, NSW, Australia
[g] ENT Department, Royal North Shore Hospital, St Leonards, NSW, Australia
[h] St Vincent's Hospital Clinical School, University of New South Wales, Sydney, NSW, Australia
[i] Griffith Institute for Drug Discovery, Griffith University, Nathan, QLD, Australia

ARTICLE INFO

ABSTRACT

Zellweger syndrome spectrum disorders are caused by mutations in any of at least 12 different *PEX* genes. This includes *PEX16*, an important regulator of peroxisome biogenesis. Using whole genome sequencing, we detected previously unreported, biallelic variants in *PEX16* [NM_004813.2:c.658G > A, p.(Ala220Thr) and NM_004813.2:c.830G > A, p.(Arg277Gln)] in an individual with leukodystrophy, spastic paraplegia, cerebellar ataxia, and craniocervical dystonia with normal plasma very long chain fatty acids. Using olfactory-neurosphere derived cells, a population of neural stem cells, we showed patient cells had reduced peroxisome density and increased peroxisome size, replicating previously reported findings in *PEX16* cell lines. Along with alterations in peroxisome morphology, patient cells also had impaired peroxisome function with reduced catalase activity. Furthermore, patient cells had reduced oxidative stress levels after exposure to hydrogen-peroxide (H_2O_2), which may be a result of compensation by H_2O_2 metabolising enzymes other than catalase to preserve peroxisome-related cell functions. Our findings of impaired catalase activity and altered oxidative stress response are novel. Our study expands the phenotype of *PEX16* mutations by including dystonia and provides further insights into the pathological mechanisms underlying *PEX16*-associated disorders. Additional studies of the full spectrum of peroxisomal dysfunction could improve our understanding of the mechanism underlying PEX16-associated disorders.

1. Introduction

PEX16 mutations are known to cause a phenotypic spectrum including Zellweger syndrome [1, 2], leukodystrophy, spastic ataxia [3, 4] and hereditary spastic paraplegia (HSP) [5]. In mammalian cells, peroxisome biogenesis factor 16, encoded by *PEX16*, is essential for de novo peroxisome synthesis [6]. Peroxisomes play multiple roles in mammalian cells including fatty-acyl-CoA metabolism (alpha- and beta-oxidation), synthesis of specialised ether lipids (plasmalogens), and redox control [7].

We performed whole genome sequencing (WGS) in a family in whom the proband had a complex neurological phenotype including leukodystrophy, spastic paraplegia, cerebellar ataxia, and craniocervical dystonia. We detected previously unreported biallelic variants in the *PEX16* gene. To determine the effect of these variants in patient cells, we evaluated peroxisome morphology and function in patient and healthy control olfactory neurosphere-derived (ONS) cells, a population of neural stem cells [8–10]. This patient-derived cell model has previously been used to model neurological disorders including HSP [10–13].

2. Materials and methods

2.1. Editorial policies and ethical considerations

The study was performed with written and informed consent of all participants and with approval from the local human ethics committees (HREC/13/RPAH/363, HREC/10/HAWKE/132). Olfactory mucosa biopsy procedures were carried out as described previously [8], in accordance with the Northern Sydney Local Health District Human Research Ethics Committee and guidelines of the National Health and Medical Research Council of Australia.

2.2. Whole genome sequencing

WGS was performed on the Illumina HiSeq X sequencers at the Kinghorn Centre for Clinical Genomics. Data was analysed following the GATK best practices pipeline, as described [5]. We investigated a panel of known leukodystrophy genes (see Supplementary Table 1), as well as filtering according to a homozygous, compound heterozygous or de novo dominant inheritance pattern. Variants were assessed according to frequency in population databases (including gnomAD [14]), predicted pathogenicity, and segregation with disease, using an inhouse platform, Seave [15]. We also interrogated for copy number variants and structural variants, using ClinSV as described [5], in genes from the leukodystrophy panel.

2.3. Cell culture

ONS cells were derived from the olfactory mucosa tissue biopsy of participants as described [10]. Details of all olfactory mucosa biopsy participants are in Supplementary Table 2. Cells were cultured in Dulbecco's Modified Eagle Medium (DMEM)/F12 (Gibco) with 10% fetal bovine serum at 37 °C and 5% CO_2.

2.4. Peroxisome morphology assay

Briefly, cells were fixed in 4% paraformaldehyde; blocked and permeabilized with 3% bovine serum albumin (Sigma) with 0.1% Triton X-100; incubated with antibodies against microtubules (1:1000, acetylated α-tubulin, Santacruz Biotechnology) and peroxisomes (1:1000, PEX14 [16, 17]); incubated with secondary antibodies (1:400, Alexa Fluor® 488 and Alexa Fluor® 594, ThermoFisher Scientific) for 30 min and stained with DAPI (1:1000; Life Technologies) to label nucleus. Microtubules were labelled to identify the total cell area.

Cells were visualized and imaged using a Leica SP5 confocal microscope (Leica, Germany) at high magnification of 60×. Resulting images were analysed for peroxisome density and size using image J image analysis software [18]. For peroxisome density, the total area of the cell and number of peroxisomes in a cell were measured. Peroxisome density was measured and reported as a ratio of number of peroxisomes to the total cell area. The analysis was performed on about 10 cells per cell line. Three controls and one *PEX16* patient cell line were used for this analysis. Peroxisome size was also calculated using ImageJ on the same cells.

2.5. Catalase activity

Catalase activity was determined using the Catalase Assay Kit (ab83464, Abcam) as per manufacturer's instructions. Briefly, cells were lysed and protein concentration of the cell lysate containing catalase was determined. Catalase decomposes H_2O_2 to water and oxygen. The assay uses the unconverted H_2O_2 and reacts with OxiRed probe to produce a product that can be measured at 570 nm.

2.6. General oxidative stress

Cells were plated at 10000 cells per well in a 96-well microplate and cultured for 24 h before measuring CM-H2DCFDA (an indicator of H_2O_2, ThermoFisher Scientific). CM-H2DCFDA staining was performed as per manufacturer's instructions. Briefly, cells were stained with 5 mM CM-H2DCFDA for 15 min at 37 °C. The cells were then washed in phosphate-buffered saline and the fluorescence was immediately measured using a Victor 3 V1420 multilabel plate counter (Perkin Elmer). The measurements were acquired for patient and control cells treated with and without H_2O_2. A sister plate was setup to normalize the CM-H2DCFDA fluorescence intensity to cell number measured using CyQUANT NF Cell Proliferation Assays (Thermofisher Scientific).

3. Results

3.1. Clinical phenotype of proband

A 41-year-old female was observed to have toe-walking and frequent trips and falls from 3 years of age. Her walking difficulties progressed, and she is now restricted to a wheelchair for mobility. She noticed an upper limb tremor and difficulty performing fine motor tasks. From the age of 19 years she developed involuntary facial movements with limited benefit from botulinum toxin injections. By her mid-thirties she developed a speech disturbance.

Clinical examination revealed mild cervical dystonia with head tilt to the right and chin rotation to the left, and a 'no no' head tremor. She also had continuous rhythmic movements of the forehead, involuntary movements of the mouth resembling Meige syndrome, intact extraocular eye movements, cerebellar dysarthria, upper limb ataxia, and marked lower limb spasticity. Cognition appeared preserved, with a mini-mental state examination score of 29/30. There was no history of seizures, liver disease, or adrenal insufficiency.
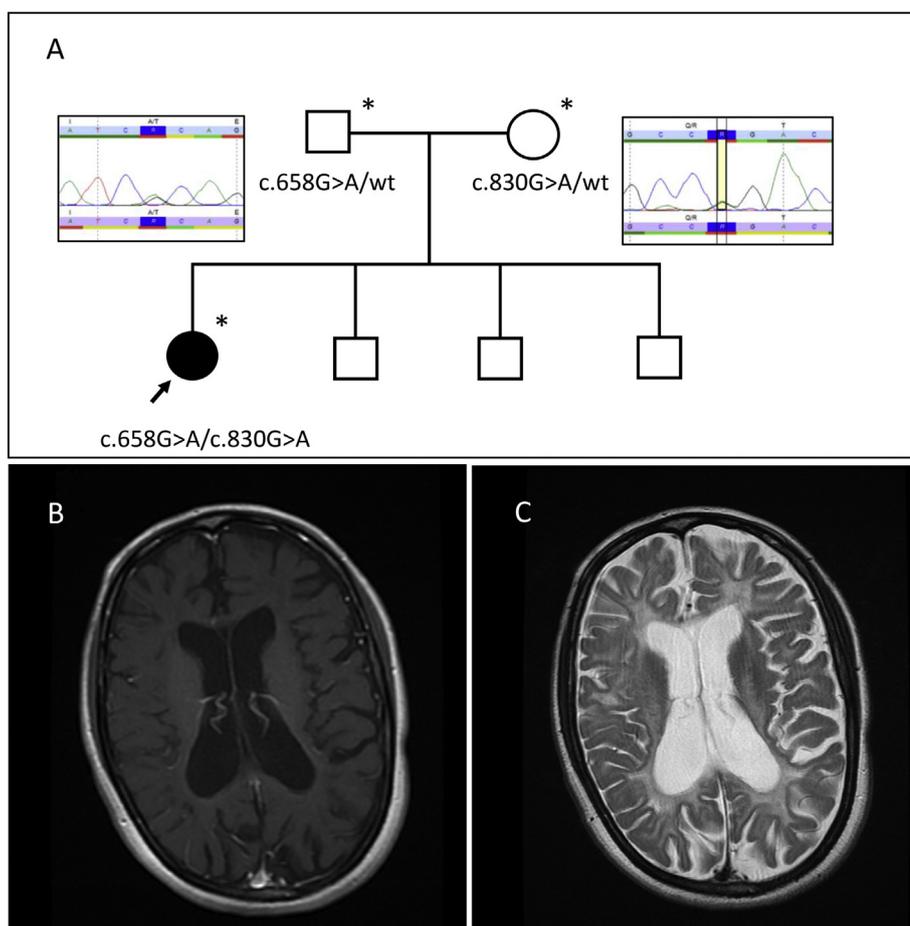
There were no other similarly affected family members (Fig. 1A). Magnetic resonance imaging of the brain showed confluent white matter changes with atrophy (Fig. 1B–C). Magnetic resonance spectroscopy (MRS) showed a raised myoinositol peak. Nerve conduction studies and needle electromyography were within normal range.

Previous genetic testing was negative including sequencing and multiplex ligation depended probe amplification of *ATL1* and sequencing of the *NIPA1* and *EIF2B1* - *EIF2B5* genes. Plasma very long chain fatty acids (VLCFA) and lysosomal enzymes were normal (Supplementary Tables 3 and 4 respectively).

3.2. WGS molecular analysis

We identified biallelic variants in the gene *PEX16* [NM_004813.2:c.658G > A, p.(Ala220Thr) and NM_004813.2:c.830G > A, p.(Arg277Gln)], not previously reported as causative of a human phenotype, as the most plausible candidate variants (Supplementary Table 5). The variants were absent [p.(Ala220Thr)] or very rare [allele frequency 0.000008247 for p.(Arg277Gln)] in the gnomAD database [14], showed species conservation, and were predicted damaging by in silico analysis (SIFT [19] and Polyphen2 [20]) with a CADD [21] score of 34 and 35 respectively. The variants appropriately segregated in the parents (Fig. 1A). The proband's siblings were not available for genetic testing.

The other candidate variants were in genes consistent with a compound heterozygous (*ADAMTSL1*, *TSTA3*) or de novo dominant (*ANO2*, *ID4*) pattern of inheritance. However, these variants were not known to be associated with human disease phenotypes. Furthermore, heterozygous de novo variants in *ANO2* and *ID4* were also found in a control sample of healthy elderly individuals [22]. However, we cannot definitively exclude that variants in these genes were contributing to the proband's phenotype.

Fig. 1. Panel A. Family pedigree. Filled indicates affected, arrow indicates proband. Whole genome sequencing was performed in individuals marked by the asterix. Relevant electropherograms of heterozygous variants shown (inset). Panel B-C. MRI images, axial T1-weighted post contrast and T2-weighted fast spin-echo respectively, showing diffuse white matter hyperintensities with atrophy.

3.3. Altered peroxisome morphology in patient cells

We investigated peroxisome morphology in patient and control cells (Fig. 2A–D). In comparison to control cells, patient cells had lower peroxisome density (Fig. 2C, control cell peroxisome density: 0.005 ± 0.0004, patient cell peroxisome density: 0.003 ± 0.0002, $t = 3.215$, df = 39, $p = .001$). Compared to controls, patient cell peroxisomes had increased size (Fig. 2D, control cell peroxisome size: $1.06 \pm 0.02\,\mu m$, patient cell peroxisome size: $1.20 \pm 0.08\,\mu m$, $t = 1.872$, df = 40, $p = .034$).

3.4. Reduced catalase activity in patient-derived cells

We investigated peroxisome function by evaluating catalase activity in patient and control cells. Compared to control cells, patient cells had lower catalase activity (Fig. 2E, control catalase activity: 5.373 ± 0.28 U/mg of protein, patient catalase activity: 3.444 ± 0.23 U/mg of protein, $t = 3.748$ df = 10, $p = .004$).

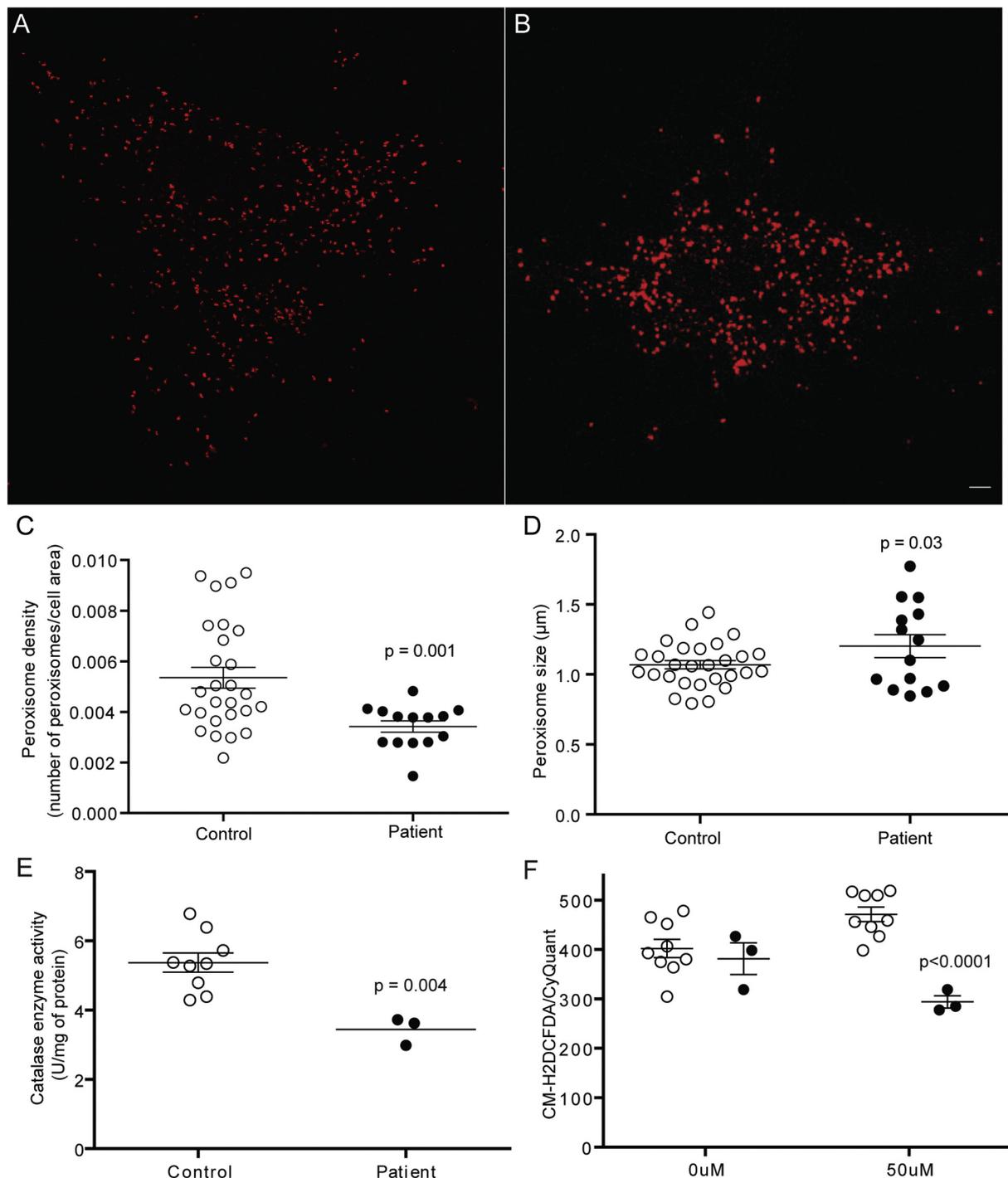### 3.5. Patient cells have reduced levels of H_2O_2 induced oxidative stress

We assessed the levels of oxidative stress using a fluorescent indicator CM-H2DCFDA in patient and control cells, with and without exposure to H_2O_2. Cells with high levels of oxidative stress have relatively higher fluorescence intensity and vice versa. The fluorescence levels were comparable between patient and control cells at basal levels when they were not exposed to H_2O_2 (Fig. 2F; control: 401.9 ± 18.44, patient: 381.2 ± 32.16). When exposed to H_2O_2, as anticipated CM-H2DCFDA fluorescence increased in control cells treated with H_2O_2 in comparison to untreated controls (Fig. 2F; Untreated controls: 401.9 ± 18.44; H_2O_2 treated controls: 470.9 ± 14.72). Contrary to

expectations, CM-H2DCFDA fluorescence decreased in patient cells treated with H_2O_2 in comparison to untreated patient cells (Fig. 2F; Untreated patient: 381.2 ± 32.16; H_2O_2 treated patient: 293.8 ± 12.77). The patient-control difference in cells exposed to H_2O_2 was significant ($p < .0001$).

4. Discussion

We detected compound heterozygous variants in the *PEX16* gene [NM_004813.2:c.658G > A, p.(Ala220Thr) and NM_004813.2:c.830G > A, p.(Arg277Gln)] in an individual with a complex neurological phenotype including leukodystrophy, spastic paraplegia, cerebellar ataxia, and craniocervical dystonia. Although traditionally peroxisome biogenesis disorders have been associated with severe disease forms such as Zellweger syndrome, more recently relatively milder atypical clinical manifestations such as ataxia and spasticity have been described for *PEX2* [23], *PEX10* [24], and *PEX16* [3–5] mutations. To our knowledge, dystonia is a newly associated manifestation that adds to the phenotypic spectrum of *PEX16*-related disorders.

MRS can be used to evaluate white matter signal abnormalities by measuring by measuring changes in brain biochemistry such as levels of myo-inositol. Myo-inositol is a glucose-like metabolism which is located within astrocytes and glial cells, and so it is a glial specific marker [25–27]. Elevation of the myo-inositol peak may be due to elevated astrocytosis and the proliferation of glia and can be seen in a variety of brain disorders such as Alzheimer's disease, gliomatosis cerebri, diabetes mellitus, recovering hypoxia, progressive multifocal leukoencephalopathy, systemic lupus erythematosus, familial hemiplegic migraine, Canavan disease, multiple sclerosis, and Alexander's leukodystrophy [25–27]. In the reported proband the myo-inositol peak was elevated, and we interpret this as a nonspecific finding of glial proliferation.

Fig.2. (A–B) Representative control cells (A) and patient cells (B) immunostained with an antibody to peroxisomes (red). (C) Peroxisome density was quantified as the ratio of peroxisome number (red fluorescence) to cell area. The peroxisome density in patient cells (black dots) is significantly reduced in comparison to control cells (white dots). Control N = peroxisome density in 27 control cells from three cell lines and 14 patient cells from one *PEX16* cell line; unpaired *t*-test; one-tailed; p-value: 0.001; $t = 3.215$, df = 39. (D) Peroxisome size in patient cells (black dots) were significantly increased in comparison to control cells (white dots). Control N = average size of peroxisomes in 27 control cells from three cell lines and peroxisomes in 14 patient cells from one *PEX16* cell line; unpaired t-test; one-tailed; p-value: 0.0342; $t = 1.872$ df = 40. (E) Catalase activity was detected in patient and control cells using the Catalase Activity Assay Kit. 1 Unit Catalase activity = amount of catalase that will decompose 1.0 μmol of H_2O_2 per minute. Catalase activity is patient cells was lower than control cells ($p = .004$). N = 3 control cell lines and a *PEX16* patient cell line. The experiment was repeated three times.(F) CM-H2DCFDA was used to detect H_2O_2 reactive oxygen species in patient and control cells. In cells, at basal levels, when not exposed to H_2O_2 the CM-H2DCFDA fluorescence intensity was comparable between patient and control cells. But, when treated with 50 μm H_2O_2 for 1 h, CM-H2DCFDA fluorescence intensity was significantly different between patient and control cells. A repeated measures analysis of variance demonstrated a significant main effect for H_2O_2 treatment ($p < .0001$), confirming the difference in patient and control cell response to H_2O_2. N = 3 control cell lines and a *PEX16* patient cell line. The experiment was repeated three times. Data are represented as Mean ± SEM. Scale bar: 5μm (For interpretation of the references to colour in this figure legend, the reader is referred to the web version of this article.)

The normal phytanic acid and pristanic acid in the proband may be consistent with normal alpha-oxidation and beta-oxidation activity respectively [28] and is in keeping with the findings from a recently described patient with mild peroxisomal biochemical abnormalities [4]. Measurement of erythrocyte plasmalogens by gas chromatography is typically included in the investigations for peroxisomal disorders to investigate for a defect in plasmalogen biosynthesis [28]. Unfortunately, erythrocyte plasmalogens could not be measured in this case. Although plasmalogen levels are low in severely affected cases of Zellweger spectrum disorder it can be completely normal in milder patients [28, 29]. This is consistent with reports of mild phenotypes of *PEX16*, where erythrocyte plasmalogen levels were normal [3, 4].

Abnormal peroxisome morphology has previously been associated with progressive spastic paraplegia patients carrying *PEX16* mutations [3]. Visual inspection of cells from six *PEX16* patient fibroblast cell lines carrying multiple mutations revealed enlarged peroxisomes and reduced number of peroxisomes [3]. These observations are consistent with our findings here, which are based on automated image analysis quantification of a large number of peroxisomes in ONS cells, a population of neural stem cells which are affected in neurological disorders.

Patient cells showed reduced catalase activity in comparison to control cells, which could be explained by the reduced number of peroxisomes in patient cells. There are many enzymes that metabolise H_2O_2 to water and oxygen including peroxiredoxin, glutathione peroxidase and peroxisome catalases. To evaluate if impaired catalase in patient cells influences their overall oxidative stress, we evaluated oxidative stress levels using CM-H2DCFDA, an indicator of oxidative stress. At basal levels, without H_2O_2 exposure, oxidative stress levels in patient and control cells were comparable. However, when challenged with H_2O_2, oxidative stress levels in patient cells were lower than control cells. This unexpected response may be due to peroxisome cell-function compensation by other H_2O_2 metabolising enzymes. Compensatory mechanisms may also explain the patient's normal plasma VLCFA and the relatively mild phenotype along the continuum of Zellweger spectrum disorders (reported here and elsewhere [3]). The findings of reduced catalase activity and altered oxidative stress response to H_2O_2 challenge have not previously been described in the context of *PEX16* mutations.

Although total cellular catalase was mildly deficient in the patient's cultured cells, this does not prove that peroxisomal catalase was mistargeted. Measurement of particulate catalase would have been more convincing of a defect in peroxisome biogenesis. Furthermore, reduced catalase activity is not likely to be the only impaired peroxisomal function in the proband; other defects may be detected with a more comprehensive analysis of peroxisomal function. For example, measurement of VLCFA content, VLCFA oxidation, phytanic acid oxidation, and plasmalogen synthesis experiments on patient cell lines may have more thoroughly documented the effect of *PEX16* mutations on peroxisomal functions. Ebberink and colleagues performed studies in *PEX16* cultured skin fibroblasts demonstrating increased levels of VLCFAs with a marginally decreased beta-oxidation rate of C26:0 in some patients [3]. They found that the phytanic acid alpha-oxidation, pristanic acid beta-oxidation and the activity of dihydroxyacetone phosphate acyltransferase were within the control range [3].

To confirm the oxidative stress response to H_2O_2, it would be useful to repeat similar experiments from cell lines of genetically proven *PEX16* cases. However, given the rarity of this disorder, we did not have access to these cell lines. Thus, the role of the *PEX16* variants could have been definitively confirmed with more comprehensive analysis of peroxisome function and by the inclusion of cell lines from additional *PEX16* cases.

Human PEX16 is an integral membrane protein that is believed to function at the endoplasmic reticulum during the earlier stages of peroxisomal formation [30]. It also recruits peroxisomal proteins directly to mature peroxisomes [30]. The exact mechanism by which it causes known features such peroxisomes increased in size and reduced

in number [3], as well as putative novel features observed in this study including reduced catalase activity, is currently unclear.

5. Conclusion

We provide evidence of a peroxisomal biogenesis disorder caused by *PEX16* mutations identified on WGS. The use of a hypothesis-free genetic testing approach allowed us to identify this disorder in the absence of typical abnormalities in peroxisomal biochemical function.

This study expands the phenotypic spectrum of *PEX16*-associated disease to include dystonia and provides novel insights into cell function defects in patient-derived cells. Although this study highlights alterations in peroxisome morphology and function in *PEX16* mutated patient cells, the mechanism underlying peroxisome dysfunction that leads to the specific clinical manifestation observed requires further investigation.

Competing interests

There are no competing interests to disclose for any of the authors.

Funding sources

Acknowledgements

Appendix A. Supplementary data

Supplementary data to this article can be found online at https://doi.org/10.1016/j.ymgmr.2018.07.003.

References

[1] M. Honsho, S. Tamura, N. Shimozawa, Y. Suzuki, N. Kondo, Y. Fujiki, Mutation in PEX16 is causal in the peroxisome-deficient Zellweger syndrome of complementation group D, Am. J. Hum. Genet. 63 (6) (1998) 1622–1630, https://doi.org/10.1086/302161.

[2] N. Shimozawa, T. Nagase, Y. Takemoto, Y. Suzuki, Y. Fujiki, R.J. Wanders, N. Kondo, A novel aberrant splicing mutation of the PEX16 gene in two patients with Zellweger syndrome, Biochem. Biophys. Res. Commun. 292 (1) (2002) 109–112.

[3] M.S. Ebberink, B. Csanyi, W.K. Chong, S. Denis, P. Sharp, P.A. Mooijer, C.J. Dekker, C. Spooner, L.H. Ngu, C. De Sousa, R.J. Wanders, M.J. Fietz, P.T. Clayton, H.R. Waterham, S. Ferdinandusse, Identification of an unusual variant peroxisome biogenesis disorder caused by mutations in the PEX16 gene, J. Med. Genet. 47 (9) (2010) 608–615, https://doi.org/10.1136/jmg.2009.074302.

[4] C. Bacino, Y.H. Chao, E. Seto, T. Lotze, F. Xia, R.O. Jones, A. Moser, M.F. Wangler, A homozygous mutation in PEX16 identified by whole-exome sequencing ending a diagnostic odyssey, Mol. Genet. Metab. Rep. 5 (2015) 15–18, https://doi.org/10.1016/j.ymgmr.2015.09.001.

[5] K.R. Kumar, G.M. Wali, M. Kamate, G. Wali, A.E. Minoche, C. Puttick, M. Pinese, V. Gayevskiy, M.E. Dinger, T. Roscioli, C.M. Sue, M.J. Cowley, Defining the genetic basis of early onset hereditary spastic paraplegia using whole genome sequencing, Neurogenetics 17 (4) (2016) 265–270, https://doi.org/10.1007/s10048-016-0495-z.

[6] M. Honsho, T. Hiroshige, Y. Fujiki, The Membrane Biogenesis Peroxin Pex16p: Topogenesis and functional roles in peroxisomal membrane assembLY, J. Biol. Chem. 277 (46) (2002) 44513–44524, https://doi.org/10.1074/jbc.M206139200.

[7] V. Antonenkov, S. Grunau, S. Ohlmeier, J. Hiltunen, Peroxisomes are oxidative organelles, Antioxid. Redox Signal. 13 (4) (2010) 525–537, https://doi.org/10.1089/ars.2009.2996.

[8] F. Féron, C. Perry, J.J. McGrath, A. MacKay-Sim, NEw techniques for biopsy and culture of human olfactory epithelial neurons, Archiv. Otolaryngol. 124 (8) (1998) 861–866, https://doi.org/10.1001/archotol.124.8.861.

[9] W. Murrell, F. Féron, A. Wetzig, N. Cameron, K. Splatt, B. Bellette, J. Bianco, C. Perry, G. Lee, A. Mackay-Sim, Multipotent stem cells from adult olfactory mucosa, Dev. Dyn. 233 (2) (2005) 496–515, https://doi.org/10.1002/dvdy.20360.

[10] N. Matigian, G. Abrahamsen, R. Sutharsan, A.L. Cook, A.M. Vitale, A. Nouwens, B. Bellette, J. An, M. Anderson, A.G. Beckhouse, M. Bennebroek, R. Cecil, A.M. Chalk, J. Cochrane, Y. Fan, F. Féron, R. McCurdy, J.J. McGrath, W. Murrell, C. Perry, J. Raju, S. Ravishankar, P.A. Silburn, G.T. Sutherland, S. Mahler, G.D. Mellick, S.A. Wood, C.M. Sue, C.A. Wells, A. Mackay-Sim, Disease-specific, neurosphere-derived cells as models for brain disorders, Dis. Model. Mech. 3 (11 − 12) (2010) 785–798, https://doi.org/10.1242/dmm.005447.

[11] G. Wali, R. Sutharsan, Y. Fan, R. Stewart, J. Tello Velasquez, C.M. Sue, D.I. Crane, A. Mackay-Sim, Mechanism of impaired microtubule-dependent peroxisome trafficking and oxidative stress in SPAST-mutated cells from patients with Hereditary Spastic Paraplegia, Sci. Rep. 6 (2016) 27004, , https://doi.org/10.1038/srep27004.

[12] R. Stewart, S. Kozlov, N. Matigan, G. Wali, M. Gatei, R. Sutharsan, B. Bellette, A. Wraith-Kijas, J. Cochrane, M. Coulthard, C. Perry, K. Sinclair, A. MacKay-Sim, M.F. Lavin, A patient-derived olfactory stem cell disease model for ataxia-telangiectasia, Hum. Mol. Genet. (2013), https://doi.org/10.1093/hmg/ddt101.

[13] R. Stewart, G. Wali, C. Perry, M.F. Lavin, F. Féron, A. MacKay-Sim, R. Sutharsan, A patient-specific stem cell model to investigate the neurological phenotype observed in ataxia-telangiectasia, in: S.V. Kozlov (Ed.), ATM Kinase: Methods and Protocols, Springer New York, New York, NY, 2017, pp. 391–400, , https://doi.org/10.1007/978-1-4939-6955-5_28.

[14] M. Lek, K.J. Karczewski, E.V. Minikel, K.E. Samocha, E. Banks, T. Fennell, A.H. O'Donnell-Luria, J.S. Ware, A.J. Hill, B.B. Cummings, T. Tukiainen, D.P. Birnbaum, J.A. Kosmicki, L.E. Duncan, K. Estrada, F. Zhao, J. Zou, E. Pierce-Hoffman, J. Berghout, D.N. Cooper, N. Deflaux, M. Depristo, R. Do, J. Flannick, M. Fromer, L. Gauthier, J. Goldstein, N. Gupta, D. Howrigan, A. Kiezun, M.I. Kurki, A.L. Moonshine, P. Natarajan, L. Orozco, G.M. Peloso, R. Poplin, M.A. Rivas, V. Ruano-Rubio, S.A. Rose, D.M. Ruderfer, K. Shakir, P.D. Stenson, C. Stevens, B.P. Thomas, G. Tiao, M.T. Tusie-Luna, B. Weisburd, H.H. Won, D. Yu, D.M. Altshuler, D. Ardissino, M. Boehnke, J. Danesh, S. Donnelly, R. Elosua, J.C. Florez, S.B. Gabriel, G. Getz, S.J. Glatt, C.M. Hultman, S. Kathiresan, M. Laakso, S. McCarroll, M.I. McCarthy, D. McGovern, R. McPherson, B.M. Neale, A. Palotie, S.M. Purcell, D. Saleheen, J.M. Scharf, P. Sklar, P.F. Sullivan, J. Tuomilehto, M.T. Tsuang, H.C. Watkins, J.G. Wilson, M.J. Daly, D.G. MacArthur, C. Exome Aggregation, Analysis of protein-coding genetic variation in 60,706 humans, Nature 536 (7616) (2016) 285–291, https://doi.org/10.1038/nature19057.

[15] Gayevskiy V, Roscioli T, Dinger ME, Cowley MJ. Seave: a comprehensive web platform for storing and interrogating human genomic variation. Bioinformatics doi: https://doi.org/10.1093/bioinformatics/bty540.

[16] T. Nguyen, J. Bjorkman, B. Paton, D. Crane, Failure of microtubule-mediated peroxisome division and trafficking in disorders with reduced peroxisome abundance, J. Cell Sci. 119 (2006) 636–645 Pt 4 https://doi.org/10.1242/jcs.02776.

[17] P. Grant, B. Ahlemeyer, S. Karnati, T. Berg, I. Stelzig, A. Nenicu, K. Kuchelmeister, D.I. Crane, E. Baumgart-Vogt, The biogenesis protein PEX14 is an optimal marker for the identification and localization of peroxisomes in different cell types, tissues, and species in morphological studies, Histochem. Cell Biol. 140 (4) (2013) 423–442, https://doi.org/10.1007/s00418-013-1133-6.

[18] C.A. Schneider, W.S. Rasband, K.W. Eliceiri, NIH Image to ImageJ: 25 years of image analysis, Nat. Methods 9 (2012) 671, https://doi.org/10.1038/nmeth.2089.

[19] P. Kumar, S. Henikoff, P.C. Ng, Predicting the effects of coding non-synonymous variants on protein function using the SIFT algorithm, Nat. Protoc. 4 (7) (2009) 1073–1081, https://doi.org/10.1038/nprot.2009.86.

[20] I.A. Adzhubei, S. Schmidt, L. Peshkin, V.E. Ramensky, A. Gerasimova, P. Bork, A.S. Kondrashov, S.R. Sunyaev, A method and server for predicting damaging missense mutations, Nat. Methods 7 (4) (2010) 248–249, https://doi.org/10.1038/nmeth0410-248.

[21] M. Kircher, D.M. Witten, P. Jain, B.J. O'Roak, G.M. Cooper, J. Shendure, A general framework for estimating the relative pathogenicity of human genetic variants, Nat. Genet. 46 (3) (2014) 310–315, https://doi.org/10.1038/ng.2892.

[22] P. Lacaze, M. Pinese, W. Kaplan, A. Stone, M.J. Brion, R.L. Woods, et al., The Medical Genome Reference Bank: a whole-genome data resource of 4,000 healthy elderly individuals. Rationale and cohort design, bioRxiv (2018), https://doi.org/10.1101/274019.

[23] C. Sevin, S. Ferdinandusse, H.R. Waterham, R.J. Wanders, P. Aubourg, Autosomal recessive cerebellar ataxia caused by mutations in the PEX2 gene, Orphan. J. Rare Dis. 6 (1) (2011) 8.

[24] Régal L, Ebberink MS, Goemans N, Wanders RJA, De Meirleir L, Jaeken J, Schrooten M, Van Coster R, Waterham HR (2010) Mutations in PEX10 are a cause of autosomal recessive ataxia. Ann. Neurol. 68 (2):259–263. doi:https://doi.org/10.1002/ana.22035.

[25] A. Nelson, R.E. Kelley, J. Nguyen, E. Palacios, H.R. Neitzschman, MRS findings in a patient with juvenile-onset Alexander's leukodystrophy, J. La State Med. Soc. 165 (1) (2013) 14–17.

[26] A. Brand, C. Richter-Landsberg, D. Leibfritz, Multinuclear NMR studies on the energy metabolism of glial and neuronal cells, Dev. Neurosci. 15 (3–5) (1993) 289–298, https://doi.org/10.1159/000111347.

[27] M. Haris, K. Cai, A. Singh, H. Hariharan, R. Reddy, In vivo mapping of brain myo-inositol, NeuroImage 54 (3) (2011) 2079–2085, https://doi.org/10.1016/j.neuroimage.2010.10.017.

[28] S. Ferdinandusse, M.S. Ebberink, F.M. Vaz, H.R. Waterham, R.J. Wanders, The important role of biochemical and functional studies in the diagnostics of peroxisomal disorders, J. Inherit. Metab. Dis. 39 (4) (2016) 531–543, https://doi.org/10.1007/s10545-016-9922-4.

[29] G. Dacremont, G. Vincent, Assay of plasmalogens and polyunsaturated fatty acids (PUFA) in erythrocytes and fibroblasts, J. Inherit. Metab. Dis. 18 (Suppl 1) (1995) 84–89.

[30] P.K. Kim, R.T. Mullen, PEX16: a multifaceted regulator of peroxisome biogenesis, Front. Physiol. 4 (2013) 241, , https://doi.org/10.3389/fphys.2013.00241.